World Electric Vehicle Journal

MDPI

Article

Sliding Mode Control of an Electric Vehicle Driven by a New Powertrain Technology Based on a Dual-Star Induction Machine

Basma Benbouya [1,*], Hocine Cheghib [1], Daniela Chrenko [2], Maria Teresa Delgado [3], Yanis Hamoudi [4], Jose Rodriguez [5] and Mohamed Abdelrahem [6,7,*]

1 Laboratory of Electromechanical Systems, Department of Electromechanics, Faculty of Technology, University of Badji Mokhtar Annaba, Annaba 23000, Algeria; hocine.cheghib@univ-annaba.dz
2 Femto-ST Institute, University of Technology of Belfort-Montbeliard, 90010 Belfort, France; daniela.chrenko@utbm.fr
3 Department of Electrical and Computer Engineering, University of Porto, 4200-465 Porto, Portugal; mto@fe.up.pt
4 Department of Electrical Engineering, Faculty of Technology, University of Bejaia, 06000 Bejaia, Algeria; yanis.hamoudi@univ-bejaia.dz
5 Center for Energy Transition, Universidad San Sebastián, Santiago 8420524, Chile; jose.rodriguezp@uss.cl
6 Electrical Engineering Department, Faculty of Engineering, Assiut University, Assiut 71516, Egypt
7 High-Power Converter Systems (HLU), Technical University of Munich (TUM), 80333 Munich, Germany
* Correspondence: basma.benbouya@univ-annaba.dz (B.B.); mohamed.abdelrahem@tum.de (M.A.)

Abstract: This article examines a new powertrain system for electric vehicles based on the dual-star induction machine, presented as a promising option due to its significant advantages in terms of performance, energy efficiency, and reliability. This system could play a key role in the evolution of electro-mobility technology. The dual-star induction machine reduces electromagnetic torque fluctuations, limits current harmonics, improves power factor, and enables half-speed operation. Our study focuses on the control strategy and operation of the traction chain for electric vehicles propelled by the dual-star induction machine (DSIM) using Matlab software with version 2017. We integrate the battery as the main energy source, along with three-level static converters for energy conversion in the vehicle's four operating quadrants. We have opted for sliding mode control, which has proven to be feasible and robust against external disturbances. Although we have modeled driver behavior, we consider it as an aspect of control, to which we add the driving profile to guide our evaluation of the control to be used for vehicle operation. The results of our study demonstrate the reliability and robustness of DSIM for electric vehicle motorization and speed control. Promoting this technology is essential to improve the overall performance and efficiency of electric vehicles, especially in traction and braking modes for energy recovery. This underscores the importance of DSIM in the sustainable development of the electric transportation system.

Keywords: electric vehicle; dual-star induction machine; three-level converter; lithium-ion battery; recovery of energy; driver's behavior model; sliding mode control

Citation: Benbouya, B.; Cheghib, H.; Chrenko, D.; Delgado, M.T.; Hamoudi, Y.; Rodriguez, J.; Abdelrahem, M. Sliding Mode Control of an Electric Vehicle Driven by a New Powertrain Technology Based on a Dual-Star Induction Machine. *World Electr. Veh. J.* **2024**, *15*, 155. https://doi.org/10.3390/wevj15040155

Academic Editor: Joeri Van Mierlo

Received: 15 February 2024
Revised: 14 March 2024
Accepted: 28 March 2024
Published: 9 April 2024

1. Introduction

Currently, atmospheric pollution, including greenhouse gas emissions, as well as global warming, pose significant challenges for humanity. Internal combustion engine vehicles are among the primary sources of greenhouse gas emissions, contributing significantly to a worldwide environmental impact [1,2]. This reality underscores the urgent need to develop cleaner and more efficient mobility solutions to mitigate this major issue of atmospheric pollution. Consequently, the promotion of electric vehicles emerges as an undeniable solution, offering significant advantages in terms of reducing pollutant emissions and noise compared to traditional vehicles [3].

A fully electric vehicle is defined as a vehicle that exclusively employs an electric motor for propulsion, a static converter for energy conversion, batteries as the primary

power source, and an electric charger for recharging. Consequently, the absence of any exhaust system on such vehicles serves as the most indicative feature of their status as vehicles with low local pollution impact [4].

In the realm of enhancing the performance of electric vehicles, research has been conducted over several decades. These endeavors predominantly focus on optimizing energy storage systems, developing charging infrastructures, as well as charging techniques and energy management during the recharging process. Rapid charging solutions have also been explored, notably through a hybridization system that combines different energy sources such as the battery, supercapacitor, and fuel cell [5–9].

On the other hand, ongoing research is also being conducted on electric machines used in the automotive sector, such as direct current machines, synchronous machines, and particularly permanent magnet synchronous machines and variable reluctance machines. These machine principles are commonly employed in the automotive market for the electrification of vehicles. The choice of machine to be installed in an electric vehicle depends on several parameters. Each range of machines has advantages and disadvantages related to production costs or procurement, as well as the desired application and defined specifications [10,11]. However, our research focuses on the utilization of a new type of machine in the automotive sector. This machine comprises a stator equipped with two identical three-phase windings and a squirrel-cage rotor. It is a dual-star induction machine known for its reliability, robustness, high efficiency, and excellent performance compared to single-star machines [12–14]. This innovative approach opens up new perspectives in the field of electric vehicle propulsion, offering a promising alternative to meet the increasing demands for performance and energy efficiency.

The objective of this study is to investigate the electrification case of a vehicle based on a dual-star induction machine and the control strategy for this type of electric vehicle with a traction chain powered by a primary and rechargeable energy source, represented by the lithium-ion battery, and a three-level static converter for electrical energy conversion to power the traction machine used in this case, representing the DSIM. This is achieved by implementing a sliding mode control with speed regulation to control and optimize the performance of the electric vehicle. This approach was chosen for its robustness against external disturbances and its ability to precisely adjust the vehicle speed in all driving phases. Furthermore, we examine various driving conditions based on the driver behavior model, which considers factors such as vehicle speed, road conditions, potential obstacles, and even driver and vehicle preferences. This comprehensive analysis covers all driving phases, from acceleration to braking, and even includes energy regeneration. This study aims to provide valuable insights for the development of advanced electric traction systems, with a focus on maximizing energy efficiency while ensuring a safe and enjoyable driving experience.

2. Materials and Methods

2.1. Dynamic Model of Electric Vehicle System

2.1.1. Dimensional Study of an Electric Vehicle

An electric vehicle is subject to a variety of forces, which must be considered throughout the design phase [15,16]. In our analysis, we took into account three main longitudinal forces that are exerting pressure on an electric vehicle with a total mass of (m) that is traveling down a slope (β) as shown in Figure 1.

The resistive force required to climb the slope (F_{slope}) depends on the slope of the road and is proportional to the mass m of the vehicle. Its expression is defined by:

$$F_{slope} = m\ g\ sin(\beta) \tag{1}$$

When a vehicle is in motion, the friction of the air on the whole of its bodywork produces an air resistance force (F_{aero}). Its expression is defined by:

$$F_{aero} = \frac{1}{2}\ \rho_{air}\ A_f\ C_d\ V_e^2 \tag{2}$$

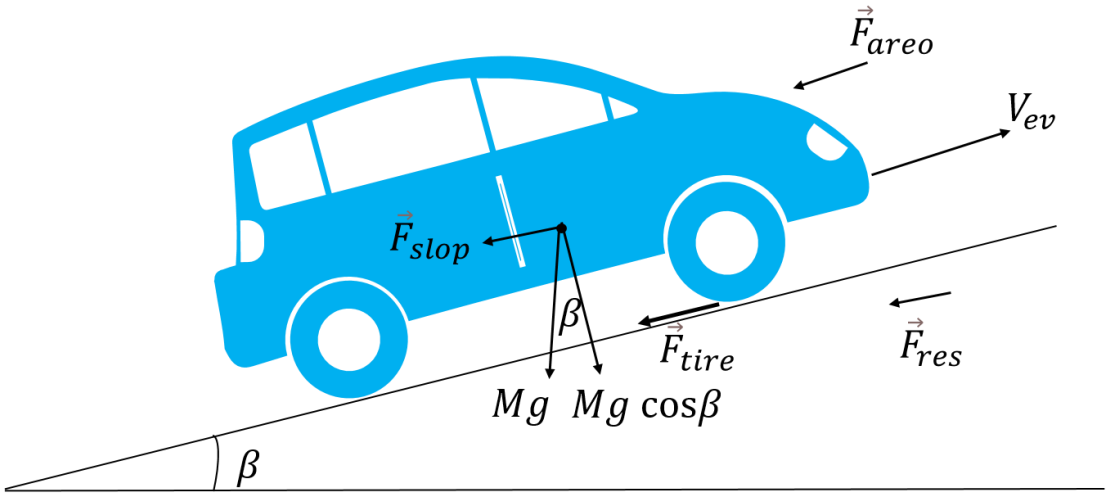

Figure 1. Typical driving force components of a vehicle.

The friction between the tires of the vehicle and the road is the primary cause of rolling resistance force (F_{tire}). Its expression is defined by:

$$F_{tire} = m\ g\ f_{ro}\ cos\ (\beta) \tag{3}$$

So, the formula for the total resistive force is:

$$F_{res} = F_{aero} + F_{tire} + F_{slope} \tag{4}$$

The electric motor provides the traction force for the electric vehicle 'F'. The equation of motion is then given by:

$$m\frac{dV_{ev}}{dt} = F - F_{res} \tag{5}$$

The mechanical power of the electric vehicle is given by:

$$P_{ev} = F_{res}\ V_e = T_{ev}\ V_e \tag{6}$$

Finally, the resistant couple is given by:

$$T_{res} = F_{res}\frac{r}{G} \tag{7}$$

2.1.2. Traction Chain

The contribution of this paper is based on the analysis of the traction system of an electric vehicle, which relies on a novel type of machine used in the automotive field. This technology incorporates the dual-star induction machine and ensures the use of three-level converters instead of conventional converters. Therefore, a detailed presentation of each component of our traction system is crucial.

So, Figure 2 represent the traction chain used in our study.

Energy Source of an Electric Vehicle

In the context of electric vehicles, the lithium-ion battery often presents the best compromise between several criteria, making it an attractive choice in the automotive industry [17–20].

- High specific energy density: Lithium-ion batteries have a high specific energy density, meaning they can store a significant amount of energy in a relatively small volume. This enables a higher range for the electric vehicle without significantly increasing its weight.

- High specific power: Lithium-ion batteries can provide high power output, which is crucial for rapid acceleration and meeting the power demands of the electric motor.
- High charge and discharge efficiency: Lithium-ion batteries exhibit high efficiency in both charging and discharging, allowing for rapid charging and efficient energy delivery to the vehicle's motor.
- Long lifespan: Compared to other battery types, lithium-ion batteries have a longer lifespan, reducing replacement costs and enhancing the overall durability of the energy storage system in the electric vehicle.
- Low self-discharge rate: Lithium-ion batteries have a relatively low self-discharge rate, meaning they can retain their charge for extended periods without requiring frequent recharging. This is advantageous for electric vehicles that may remain unused for prolonged periods.
- Established technology: Lithium-ion batteries are widely used across various industries, resulting in well-developed manufacturing and recycling infrastructure, as well as extensive knowledge regarding their usage and maintenance.

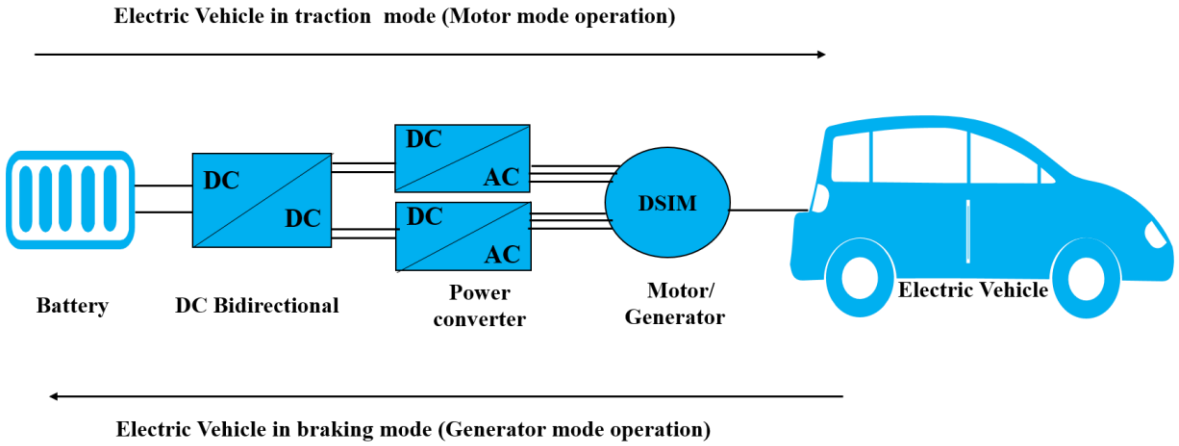

Figure 2. Schematical presentation of the traction chain of an electric vehicle.

Due to these advantages, the lithium-ion battery is often considered the preferred option for electric vehicles, offering a balanced combination of performance, range, durability, and weight. This makes it a logical choice as the energy source for electric vehicles in our study [8,17–19]. The following equations represent the charging and discharging state of the lithium-ion battery used in our study

$$V_{ch} = E_0 + K\frac{Q}{Q - it}it + k\frac{Q}{it - 0.1Q}i + Ri + Ae^{(-B.it)} \quad (8)$$

$$V_{dch} = E_0 + K\frac{Q}{Q - it}it + k\frac{Q}{Q - 0.1it}i + Ri + Ae^{(-B.it)} \quad (9)$$

Static Converters of an Electric Vehicle

In an electric vehicle powertrain, the use of static converters to convert, control, and manage electrical energy is essential. These converters play a crucial role in optimizing the energy efficiency of the vehicle and its ability to meet the requirements of clean mobility. Our study focuses on the use of three types of three-level converters, which offer a number of significant advantages. These include efficient conversion of electrical energy while reducing energy losses and improving the quality of the power supplied to the vehicle's propulsion system. Their multi-level design offers better signal quality, reduces current and voltage harmonics, and enables more precise control of electrical power. In addition, these converters offer greater flexibility in energy management, enabling the vehicle's performance to be optimized under different driving conditions [20–22].

In our study, we aim to fully exploit the advantages of this technology to improve the energy efficiency, performance, and durability of electric vehicles. By integrating these converters into the vehicle powertrain, we aim to maximize the use of electrical energy while minimizing losses, thereby contributing to more sustainable and environmentally friendly mobility [22].

- DC/DC Bidirectional converter is used for energy management and energy conversion in both directions, traction and braking.
- DC/AC converter is used to transform the energy stored in the battery into electrical energy suitable for operating the vehicle's electric motor during towing and to provide real-time control of motor speed and torque, enabling precise power management and optimized efficiency.
- AC/DC converter is used to transfer the motor's kinetic energy into electrical energy stored in the battery during braking and to control the battery's charging voltage and current, essential for efficient and safe battery recharging.

Motorization of an Electric Vehicle

Currently, existing electric vehicles on the market primarily use permanent magnet synchronous motors or variable-reluctance motors for propulsion. However, our study proposes a new approach by advocating for the use of the dual-star induction machine (DSIM) for electric vehicle propulsion. This technology promises high reliability and superior efficiency compared to motors traditionally used in the automotive industry. This choice is motivated by several criteria, including the following [23–26].

- DSIMs offer high energy efficiency, contributing to a greater electric vehicle range.
- DSIMs provide high power and torque, essential for optimal performance in terms of acceleration and load capacity.
- DSIMs are known for their reliability and longevity, reducing the risk of breakdowns and maintenance costs.
- DSIMs have a relatively simple design compared to other types of electric machines, which facilitates their integration into vehicle propulsion systems.
- DSIMs offer precise control of speed and torque, allowing them to effectively adapt to variations in load and speed encountered during driving.

Therefore, the integration of DSIMs into electric vehicles offers an attractive alternative in terms of performance, reliability, and energy efficiency, thus significantly contributing to the advancement of electro-mobility technology. Our study focuses on the adoption of this type of machine for electric vehicle propulsion, thereby proposing an innovative solution to the motorization challenges currently encountered in electric vehicles.

a. Representation of the machine

The machine we are working on is of the asynchronous type. It consists of a stator composed of two three-phase windings offset by an electrical angle (α) and a squirrel-cage rotor, which contributes to the machine's simplicity, reliability, and robustness [24–26].

This configuration corresponds to the dual-star induction machine, which has been proposed in our study to powering electric vehicles because of its unique advantages in high-power systems, particularly in the automotive sector.

b. Machine Modeling

The schematic representation of the dual-star induction machine in Figure 3 shows the position of the winding axes of the nine phases that make up the machine [25,26].

- Stator windings: The DSIM stator is divided into two sets of windings, often referred to as "star 1" and "star 2". Each set comprises three phases, giving a total of six stator phases.
- Rotor windings: The DSIM rotor also comprises three phases. These rotor windings interact with the stator's magnetic field and contribute to the machine's operation.

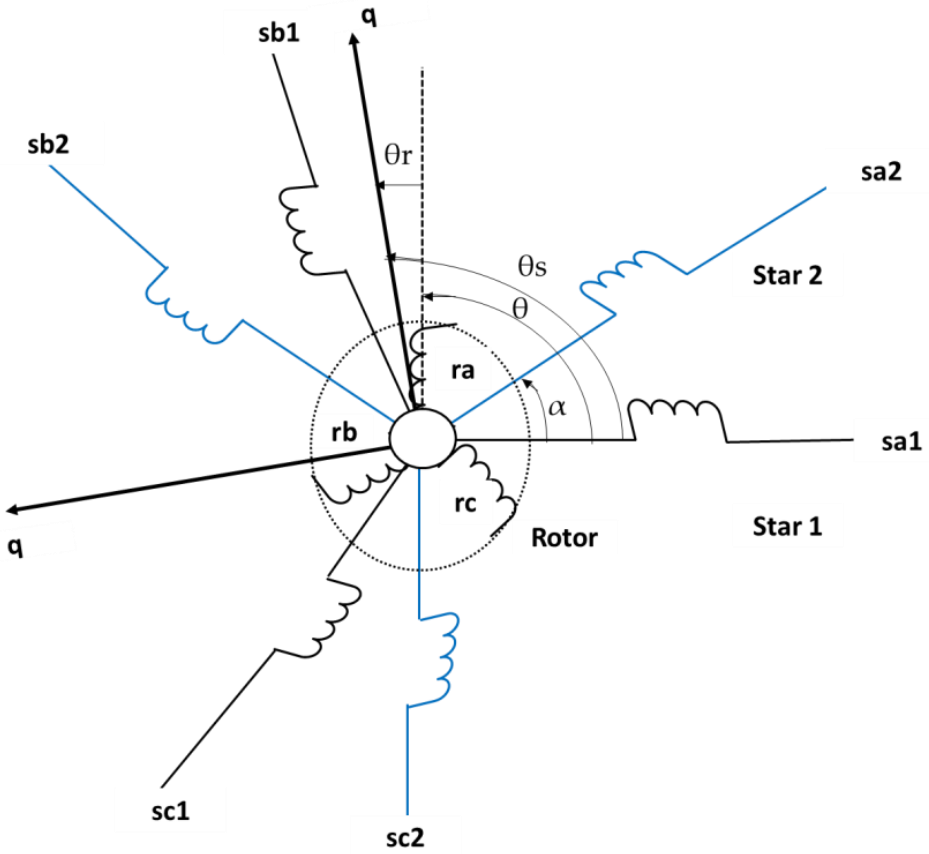

Figure 3. Representation of the machine's windings.

The mathematical representation of the DSIM associated with the "d,q" axis system after applying the Park transformation to the stator voltages is expressed by Equation (10):

$$[B][\mathrm{U}] = [\mathrm{L}][i] - \omega_s[\mathrm{D}][\mathrm{I}] - \omega_{gl}[\mathrm{C}][\mathrm{I}] + [\mathrm{R}][\mathrm{I}] \quad (10)$$

With:

$$[U] = \left[v_{ds1}, v_{qs1}, v_{ds2}, v_{qs2}, v_{dr}, v_{qr}\right]^t : \text{Controlvector}$$

$$[I] = \left[I_{ds1}, I_{qs1}, I_{ds2}, I_{qs2}, I_{dr}, I_{qr}\right]^t : \text{Statevector}$$

$$[i] = \left[i_{ds1}, i_{qs1}, i_{ds2}, i_{qs2}, i_{dr}, i_{qr}\right] : \text{Currentvector}$$

$$[B] = diag[1\ 1\ 1\ 1\ 0\ 0] : \text{Diagonalmatrix}$$

$$[R] = diag\left[R_{s1}R_{s1}R_{s2}R_{s2}R_rR_r\right] : \text{Diagonalresistancematrix}$$

$$[L] = \begin{bmatrix} (L_{s1}+L_m) & 0 & L_m & 0 & L_m & 0 \\ 0 & (L_{s1}+L_m) & 0 & L_m & 0 & L_m \\ L_m & 0 & (L_{s2}+L_m) & 0 & L_m & 0 \\ 0 & L_m & 0 & (L_{s2}+L_m) & 0 & L_m \\ L_m & 0 & L_m & 0 & (L_r+L_m) & 0 \\ 0 & L_m & 0 & L_m & 0 & (L_r+L_m) \end{bmatrix}$$

$$[D] = \begin{bmatrix} 0 & (L_{s1}+L_m) & 0 & L_m & 0 & L_m \\ -(L_{s1}+L_m) & 0 & -L_m & 0 & -L_m & 0 \\ 0 & L_m & 0 & (L_{s2}+L_m) & 0 & L_m \\ -L_m & 0 & -(L_{s2}+L_m) & 0 & -L_m & 0 \\ 0 & 0 & 0 & 0 & 0 & 0 \\ 0 & 0 & 0 & 0 & 0 & 0 \end{bmatrix}$$

$$[C] = \begin{bmatrix} 0 & 0 & 0 & 0 & 0 & 0 \\ 0 & 0 & 0 & 0 & 0 & 0 \\ 0 & 0 & 0 & 0 & 0 & 0 \\ 0 & 0 & 0 & 0 & 0 & 0 \\ 0 & -L_m & 0 & L_m & 0 & (L_r + L_m) \\ -L_m & 0 & -L_m & 0 & -(L_r + L_m) & 0 \end{bmatrix}$$

2.2. Control of the Electric Vehicle

The integration of control technology into the traction system, particularly during acceleration and deceleration, is essential to the smooth operation of the electric vehicle. Control of our powertrain is therefore of paramount importance in analyzing the operation of our machine in the automotive field, and it also enables us to detect the advantages of using DSIMs in electric vehicles. In our study, we have chosen sliding mode control for the traction system of an electric vehicle due to its numerous advantages [27–29].

- Precision: It enables precise control of the system, ensuring optimal performance of the electric vehicle in terms of acceleration, deceleration, and speed maintenance.
- Stability: It ensures robust stability, even in the presence of external disturbances or parameter uncertainties, ensuring stable operation of the vehicle in various driving conditions.
- Simplicity: It is straightforward to implement and adjust, facilitating its integration into the electric vehicle's control system.
- Responsiveness: It provides quick responses to changes in driving conditions, allowing for dynamic and effective adaptation to user commands.
- Robustness: It is renowned for its robustness against variations in system parameters and external disturbances, ensuring reliable control of the electric vehicle even in challenging environments.

2.2.1. Control Principle

Sliding mode control, belonging to the family of variable structure controllers, is a control method used to maintain a dynamic system on a specific surface known as the sliding surface. This approach is based on defining a sliding surface based on key properties such as existence, convergence, and stability. These properties act as constraints, ensuring system robustness against disturbances and uncertainties during the operation of the electric vehicle [28–30].

The explanatory diagram for the proposed vehicle traction chain control is presented in Figure 4.

2.2.2. Control Equations

During sliding mode and in steady state, we have: ($s\ (i_{ds1}) = 0$, $s\ (i_{qs1}) = 0$, $s\ (i_{ds2}) = 0$, $s\ (i_{qs2}) = 0$), and ($ps\ (i_{ds1}) = 0$, $s\ (i_{qs1}) = 0$, so the expressions of the equivalent commands are, respectively, as follows:

$$v_{d1eq} = L_{s1}\ pi_{refds1} + R_{s1}\ i_{ds1}\ - w_{refs}(L_{s1}\ i_{qs1} + \tau_r \varphi_{refr}\ w_{refgl}) \quad (11)$$

$$v_{q1eq} = L_{s1}\ pi_{refqs1} + R_{s1}\ i_{qs1}\ - w_{refs}(L_{s1}\ + i_{ds1}\varphi_{refr}\ ) \quad (12)$$

$$v_{d2q} = L_{s2}\ pi_{refds2} + R_{s2}\ i_{ds2}\ - w_{refs}(L_{s2}\ i_{qs2} + \tau_r]\varphi_{refr}) \quad (13)$$

$$v_{q2eq} = L_{s2}\ pi_{refqs2} + R_{s2}\ i_{qs2}\ - w_{refs}(L_{s1}\ i_{qs1} + \varphi_{refr}\ ) \quad (14)$$

With:

$s\ (i_{ds1})$, $s\ (i_{qs1})$, $s\ (i_{ds2})$, and $s\ (i_{qs2})$: Controlsurface

$ps\ (i_{ds1})$, $ps\ (i_{qs1})$, $ps\ (i_{ds2})$, and $ps\ (i_{qs2})$: Derivedfromcontrolsurface

During the convergence mode, we have the condition: $(s\ (i_{ds1})\ ps\ (i_{ds1}) < 0, s\ (i_{qs1})\ ps\ (i_{qs1})0, s\ (i_{ds2})\ ps\ (i_{ds2}) < 0,\ s\ (i_{qs2})\ ps\ (i_{qs2}) < 0,)$, which must be verified.

With:

$$ps\ (i_{ds1}) = -\frac{1}{L_{s1}} v_{d1n}$$

$$ps\ (i_{qs1}) = -\frac{1}{L_{s1}} v_{q1n}$$

$$ps\ (i_{ds2}) = -\frac{1}{L_{s2}} v_{d2n}$$

$$ps\ (i_{qs2}) = -\frac{1}{L_{s2}} v_{q2n}$$

We have the final equations as:

$$v_{d1n} = K_{ds1} \frac{s(i_{ds1})}{|s(i_{ds1})| + \varepsilon_{ds1}} \tag{15}$$

$$v_{q1n} = K_{qs1} \frac{s(i_{qs1})}{|s(i_{qs1})| + \varepsilon_{qs1}} \tag{16}$$

$$v_{d2n} = K_{ds2} \frac{s(i_{ds2})}{|s(i_{ds2})| + \varepsilon_{ds2}} \tag{17}$$

$$v_{q2n} K_{qs2} \frac{s(i_{qs2})}{|s(i_{qs2})| + \varepsilon_{qs2}} \tag{18}$$

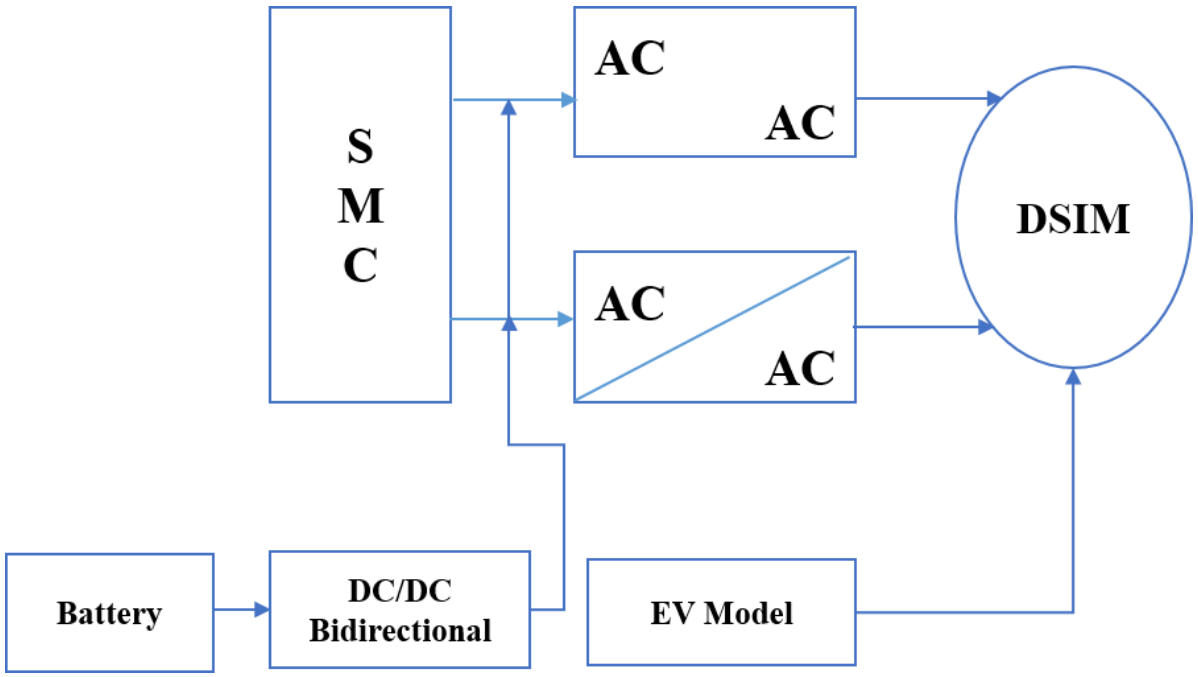

Figure 4. Sliding mode control diagram for electric vehicle.

3. Results and Discussion

After completing the implementation of the comprehensive functional schematic of the proposed traction system for an electric vehicle under sliding mode control in the Matlab/Simulink environment, utilizing the real parameters of an electric vehicle as described in Table 1, and considering the inertia moment calculated from the electric vehicle parameters (Table 1) via SolidWorks, simulations were conducted under various conditions to assess both the efficiency of the proposed powertrain and the effectiveness of the control. Special attention was given to the performance of the electric machine employed for the propulsion of the electric vehicle in this study.

Table 1. Parameters of electric vehicle.

Parameters	Values
Mass of the vehicle	$m = 1300$ kg
Wheel radius	$r = 0.32$ m
Frontal area	$A_f = 2.6$ m^2
Resistance force constant	$f_{r0} = 0.01$
The density of the air	$\rho_{air} = 1.2$ kg/m^3
Aerodynamic drag coefficients	$C_d = 0.32$
Vehicle dimensions:	4 m/1.8 m/1.6 m

Due to the extended duration of simulations and the complexity of the real-time simulation of an electric vehicle, we opted for a simulation duration of 60 s. This allowed us to study the vehicle's behavior under various conditions. The simulations considered a standardized driver behavior model, road type, speed, acceleration, and vehicle weight. These tests provided us with a detailed analysis of the operation of our electric propulsion system and enabled us to identify the performance of the electric machine in an electric vehicle under sliding mode control.

3.1. Simulation Results of Test 1: Speed Variation

This test aims to study the dynamic behavior of an electric vehicle during traction and speed variation on a flat surface under control in sliding mode. The test also aims to evaluate the efficiency of a dual-star induction machine under traction conditions involving large speed variations and analyze the characteristics of the battery with the use of three-level converters.

This test begins with a stop phase lasting 3 s, followed by an acceleration phase to 80 km/h of 8 s after a stabilization phase lasting 3 s, and a deceleration phase to 0 km/h of 6 s, followed by another stability and stop phase lasting 5 s, after another acceleration phase at 100 km/h of 10 s, followed by a stabilization phase lasting 3 s, after a deceleration phase at 60 km/h of 4 s, followed by a stabilization phase lasting 4 s, after continued deceleration with a stop phase from second 52 s.

The simulation results of this test under the Matlab Simulink environment are represented in Figure 5.

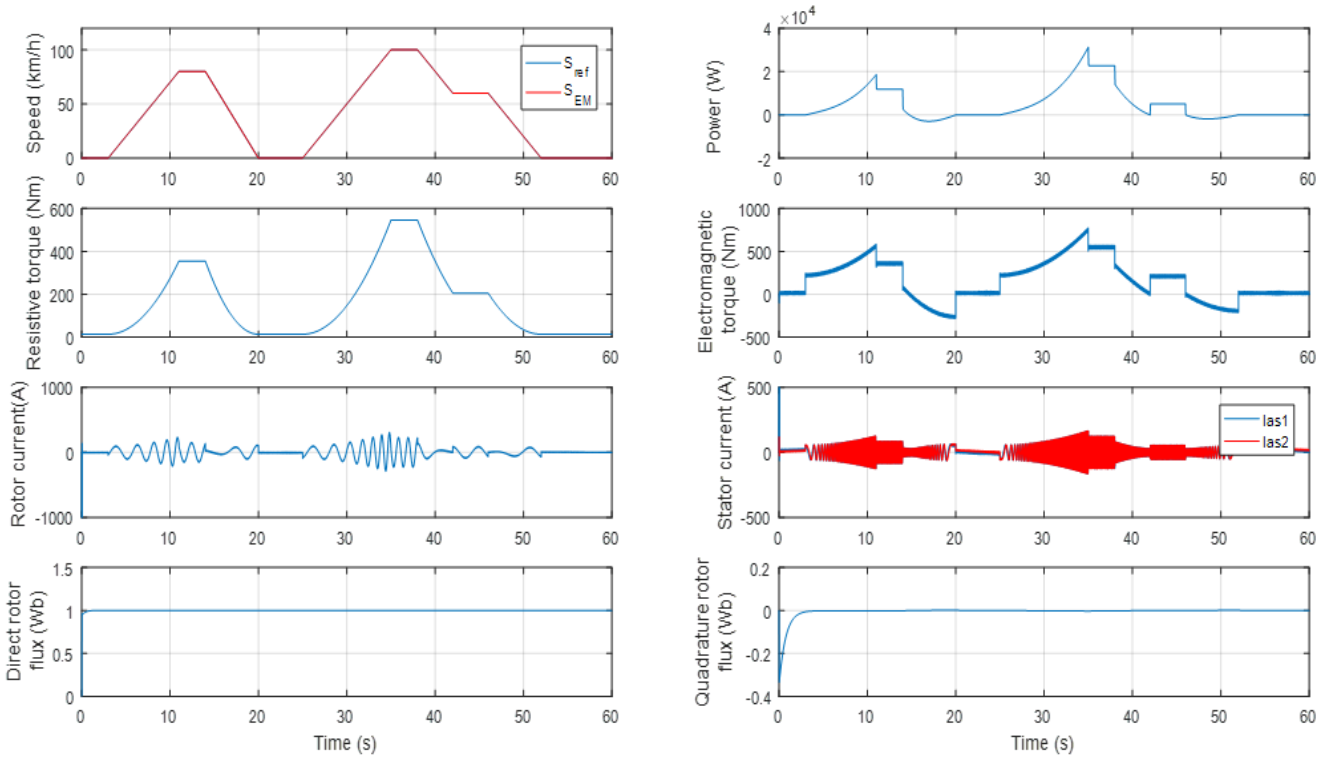

(**a**)

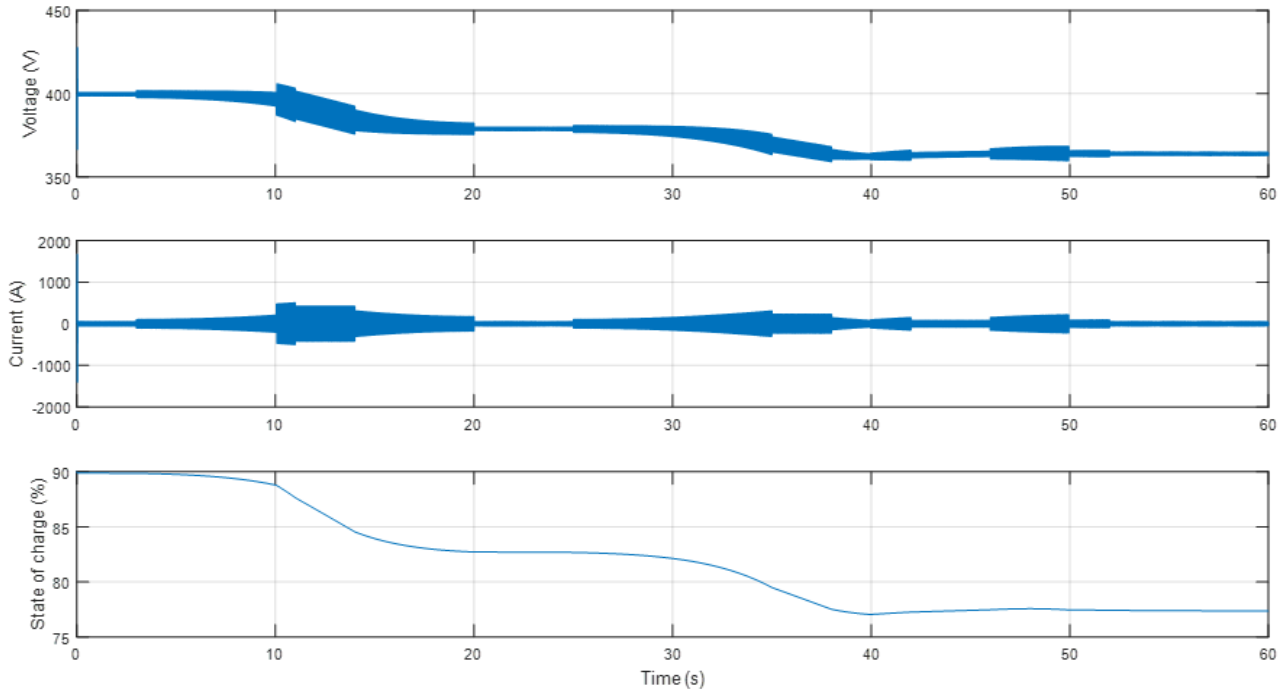

(**b**)

Figure 5. (**a**). Simulation results of test 1: Characteristic of the EV. (**b**). Simulation results of test 1: Characteristic of the battery.

From the results shown in the previous graphs, we can say the following.

During periods of standstill (0–3 s, 20–25 s, and 52–60 s), the vehicle remains immobile, characterized by minimal stator currents indicative of magnetizing current. Between 3 and 11 s, the vehicle undergoes acceleration from 0 to 80 km/h, marked by increasing currents facilitating traction torque generation. From 11 to 14 s, the vehicle reaches a steady speed, resulting in stabilized currents. During the 14 to 20 s interval, deceleration occurs, accompanied by reversed currents as the machine transitions to generator mode to replenish the battery. Subsequently, between 25 and 35 s, the vehicle undergoes acceleration again, with currents displaying a similar pattern. Between 35 and 38 s, the vehicle maintains a constant velocity mirrored by stable currents. Following this, from 38 to 42 s, deceleration occurs, leading to a reversal in currents for battery recharging purposes. The vehicle then stabilizes at a constant speed between 42 and 46 s. Finally, from 46 to 52 s, further deceleration is observed, accompanied by reversed currents to recharge the battery.

We can summarize the various modes of traction, braking, and stopping of the electric vehicle studied in this test, along with the role of the battery at each stage and the associated performance, in Table 2.

Table 2. Simulation results of test 1.

Time (s)	[3, 11]	[11, 14]	[14, 20]	[20, 25]	[25, 35]
Speed (km/h)	0–80	80	80–0	0	0–100
Traction mode	Motor	Motor	Generator	Stop	Motor
Battery state	Discharging	Discharging	Charging	Stable	Discharging
Time (s)	[35, 38]	[38, 42]	[42, 46]	[46–52]	[52, 60]
Speed (km/h)	100	100–60	60	60–0	0
Traction mode	Motor	Generator	Motor	Generator	Stop
Battery state	Discharging	Charging	Discharging	Charging	Stable

From the findings we have gathered, our conclusion is that the dual star induction machine used in this application lies in its ability to manage speed variations effectively, as well as in its capacity for optimal energy recovery stored in the batteries during the braking; this is achieved through the utilization of a three-stage converter, which greatly enhances the energy efficiency and overall performance of the powertrain of the vehicle.

3.2. Simulation Results of Test 2: Speed Reversal

In this test, we have treated a reversing cycle with sliding mode control, which represents the case of a forward speed and a reverse speed on a straight road, to study the dynamic behavior of the electric vehicle during forward and reverse traction. We are focusing in particular on the behavior of the dual-star induction machine and the characteristics of the battery during the reduction in its state of charge due to its use for driving the electric vehicle in both directions.

- Forward speed: starts with a stop phase of 3 s, followed by an acceleration phase to 80 km/h of 8 s after a stabilized phase lasting 10 s, and deceleration to 0 km/h of 8 s with a stop phase of 10 s.
- Reverse speed: starts with the last stop phase followed by an acceleration phase to 20 km/h of 3 s after a stabilized phase lasting 8 s, and deceleration to 0 km/h of 3 s with a stop phase from the second 53.

The simulation results of this test under the Matlab Simulink environment are represented in Figure 6.

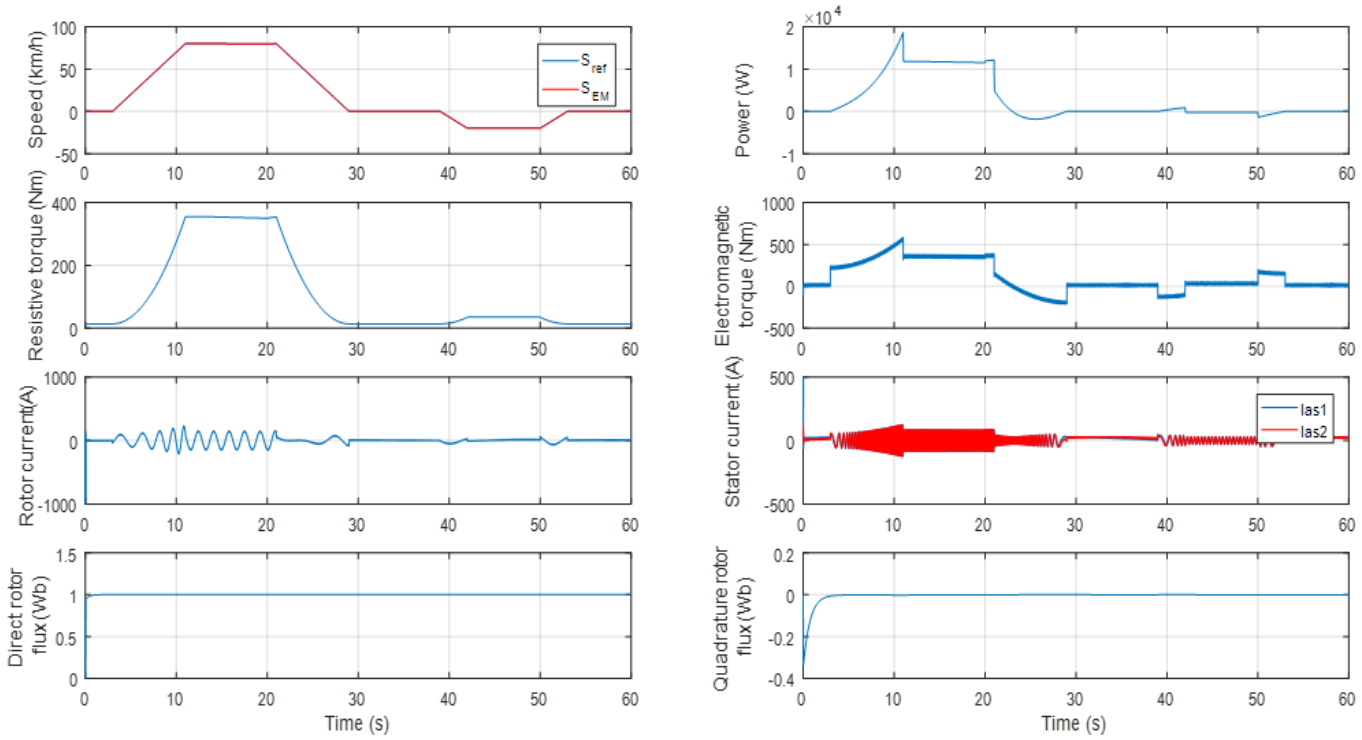

(**a**)

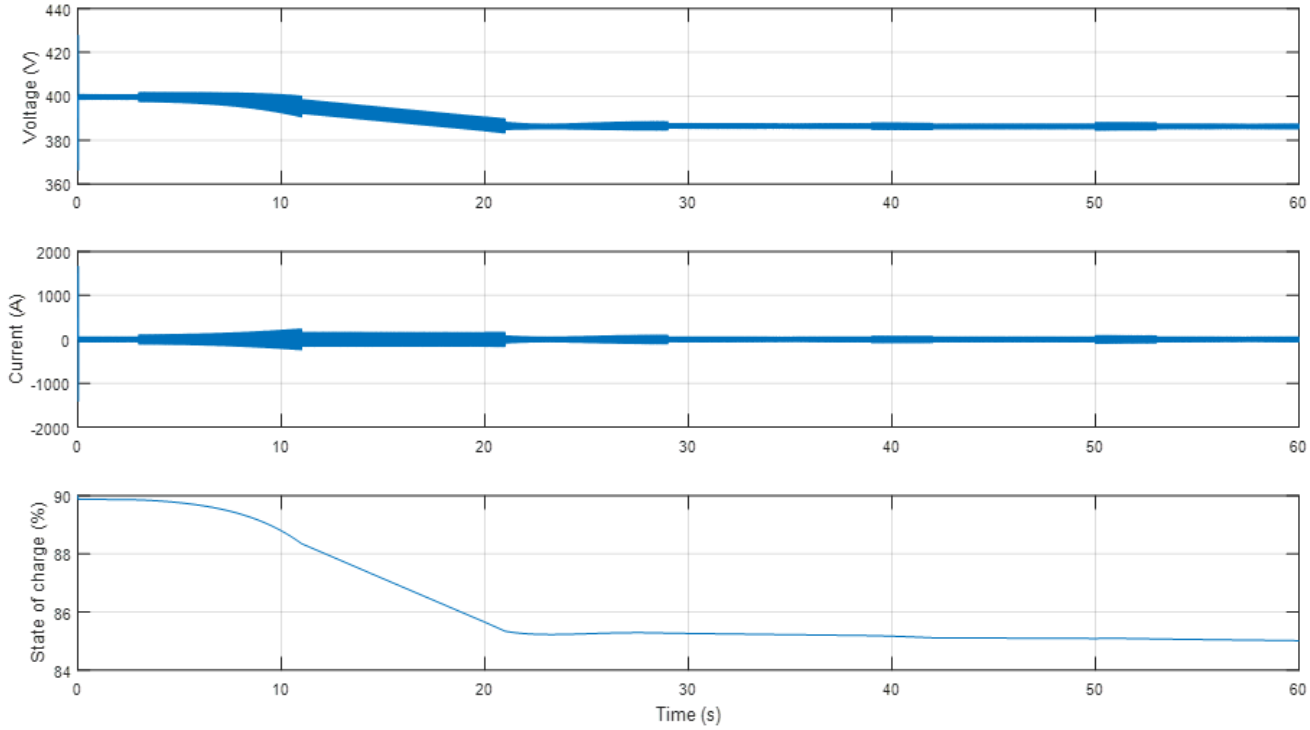

(**b**)

Figure 6. (**a**). Simulation results of test 2: Characteristic sizes of the EV. (**b**). Simulation results of test 2: Characteristic of the battery.

The simulation results of this test can be used to summarize the power results, as shown in Figure 7, where the sign of the power determines the direction of energy transfer between the sources and the machine, which shows the operation of the electric vehicle in four quadrants.

- The first quadrant represents system operation in a motor mode in the forward direction. Power is positive (Ωm > 0 Cem > 0), which means the system is consuming energy. Energy is transferred from the sources to the motor.
- The second quadrant corresponds to operation in a generator or braking mode in the forward direction. Power is negative (Ωm > 0 Cem < 0), which means the system is producing energy. Energy is transferred from the motor to the sources.
- The third quadrant represents system operation in a motor mode in reverse. Power is positive (Ωm < 0 Cem < 0), indicating energy consumption.
- Energy is again transferred from the sources to the motor.
- The fourth quadrant corresponds to operation in generator mode or braking in reverse. Power is negative (Ωm < 0 Cem > 0), meaning that the system is generating energy. Energy is transferred from the motor to the sources.

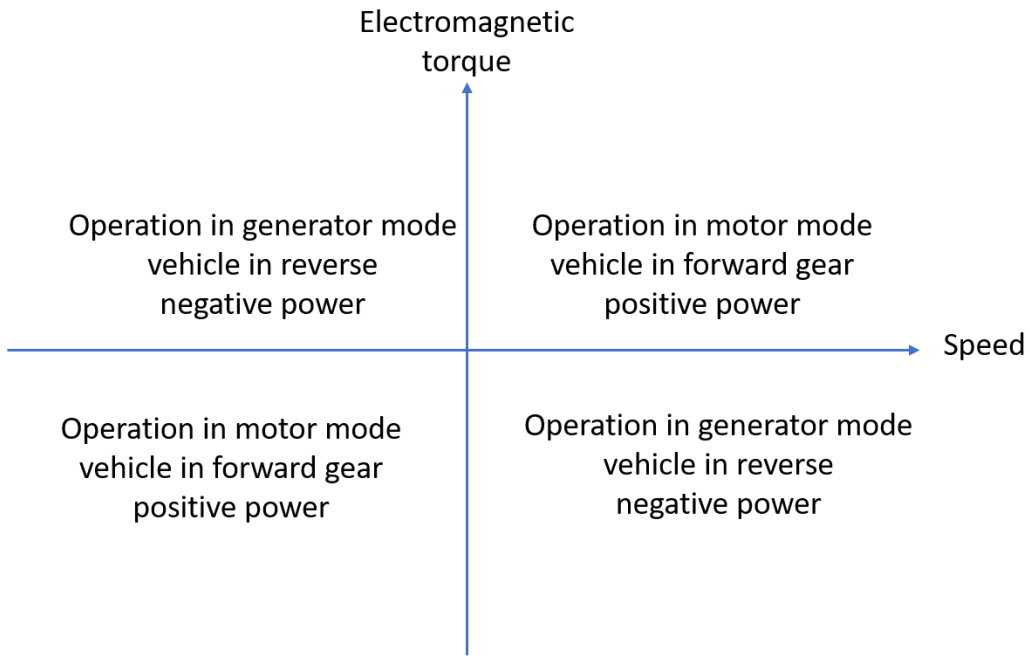

Figure 7. Power of electric vehicle.

From these results, we conclude that the dual-star induction machine provides optimum power in both directions of energy transfer between the sources and the machine, which is ideal for the overall operation of the electric vehicle in all four quadrants, so the use of this machine configuration for electric vehicle traction is robust and reliable.

3.3. Simulation Results of Test 3: Slope Variation

This test is for the purpose of studying the dynamic state of the electric vehicle under sliding mode control when pulled on different gradients and also to study the performance of the dual-star inductor machine and the battery characteristics during this variable road condition.

We take a stabilized speed of 80 km/h from second 3 and apply a bridge where the vehicle tackles an uphill slope with a gradient of 30% from second 10 s to second 20 s, followed by a downhill slope of 15% from second 40 s to second 50 s. The simulation results of this test under the Matlab Simulink environment are represented in Figure 8.

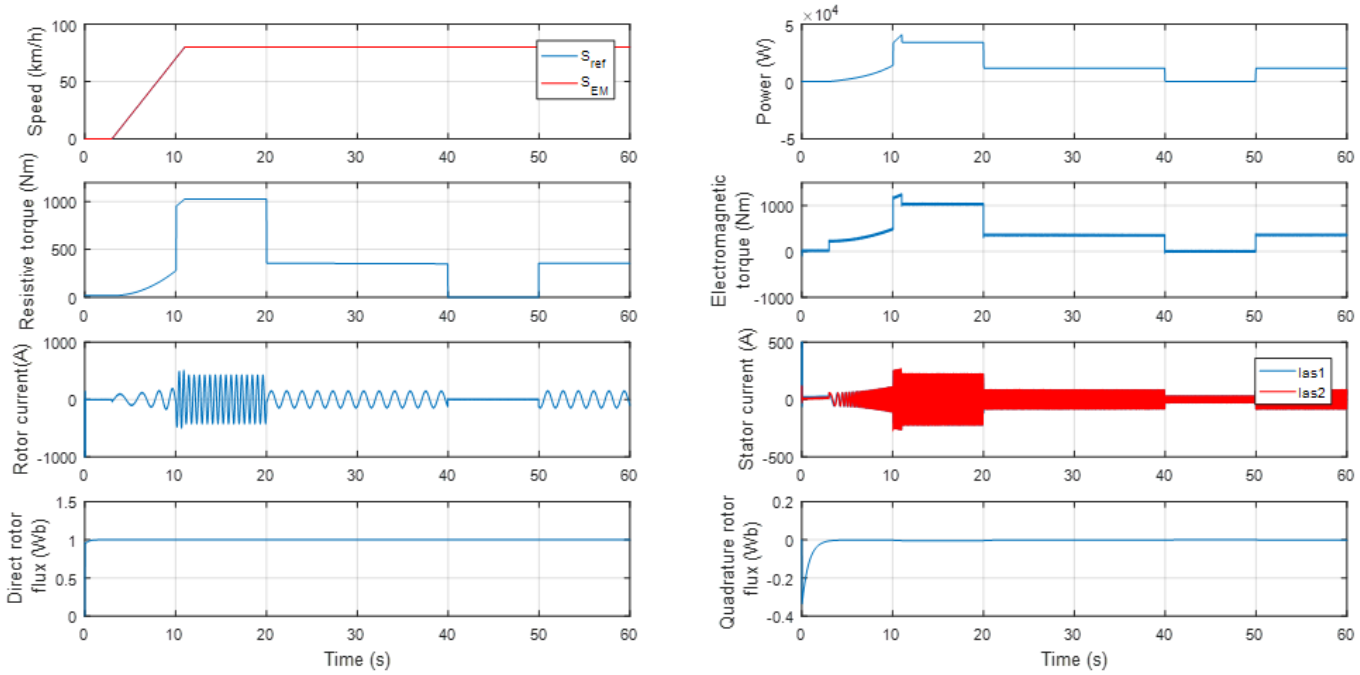

(**a**)

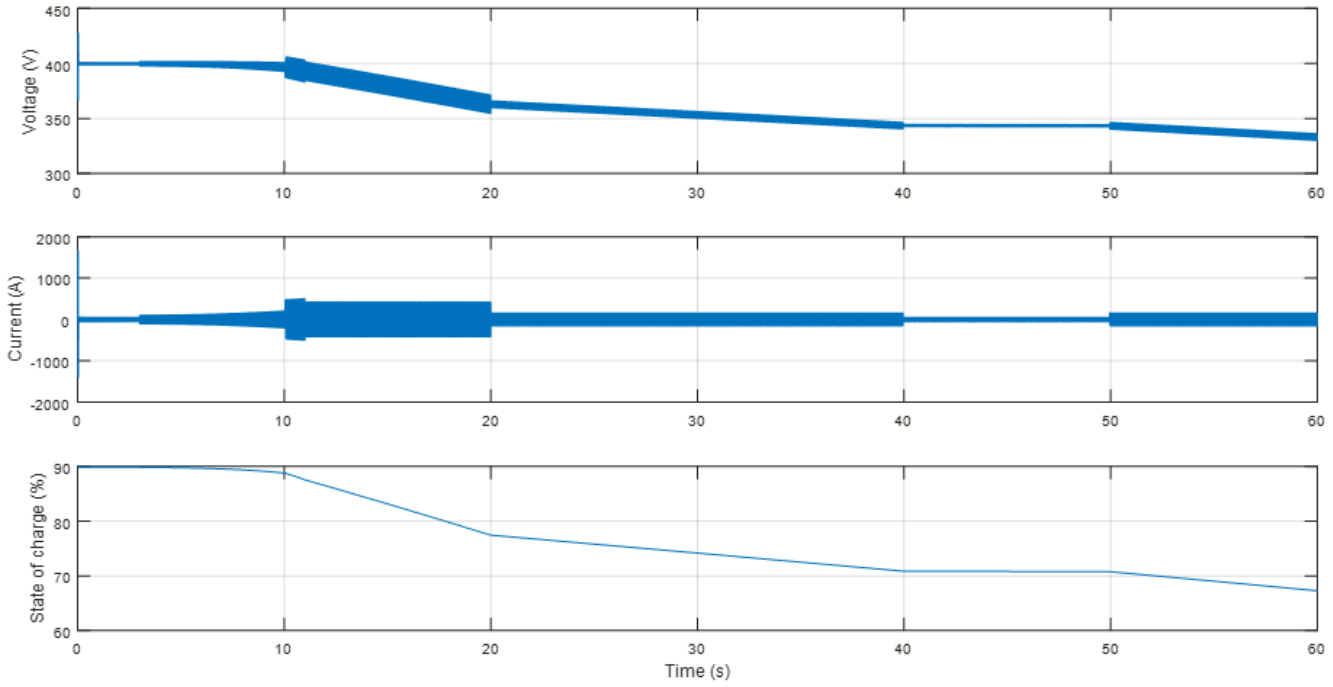

(**b**)

Figure 8. (**a**). Simulation results of test 3: Characteristic of the EV. (**b**). Simulation results of test 3: Characteristic of the battery.

The results of the simulation of this test show that the electromagnetic torque generated by the machine follows the resistive torque of the electric vehicle and follows the profile of the road, the latter deciding on the energy required to pull the vehicle.

- From 10 s to 20 s, while the vehicle is climbing 30%, the EV requires a very high level of energy, so it can triple the energy consumed during traction on a straight road.
- From 40 s to 50 s, when the vehicle is decelerating by 15%, the EV supplies minimal energy during traction and about the gradient.

As these results demonstrate, the dual-star induction machine and three-stage converter in the vehicle are reliable, ensuring reliable performance and adaptive power management to overcome the challenges encountered on gradients.

3.4. Simulation Results of Test 4: Load Increase

This test is for the dynamic state of the electric vehicle driven by the dual-star induction machine under control in sliding mode when the mass of the EV is overloaded, as well as the characteristics of the battery, which represent a reduction in the state of charge due to its use for traction of the vehicle during the variation of the slope and the overloading of the vehicle.

We carried out this test during an acceleration phase from second 3 to second 11 after a steady state with an increase in the vehicle load, bearing in mind that the vehicle weight is 1300 kg unlading with the driver, and in this test, we added a load weight of up to 700 kg so that the vehicle load becomes 2000 kg to the vehicle weight, and the vehicle tackles an uphill gradient of 30% from second 10 to second 20 and a downhill gradient of 15% from second 40 to second 50.

The simulation results of this test under the Matlab Simulink environment are represented in Figure 9.

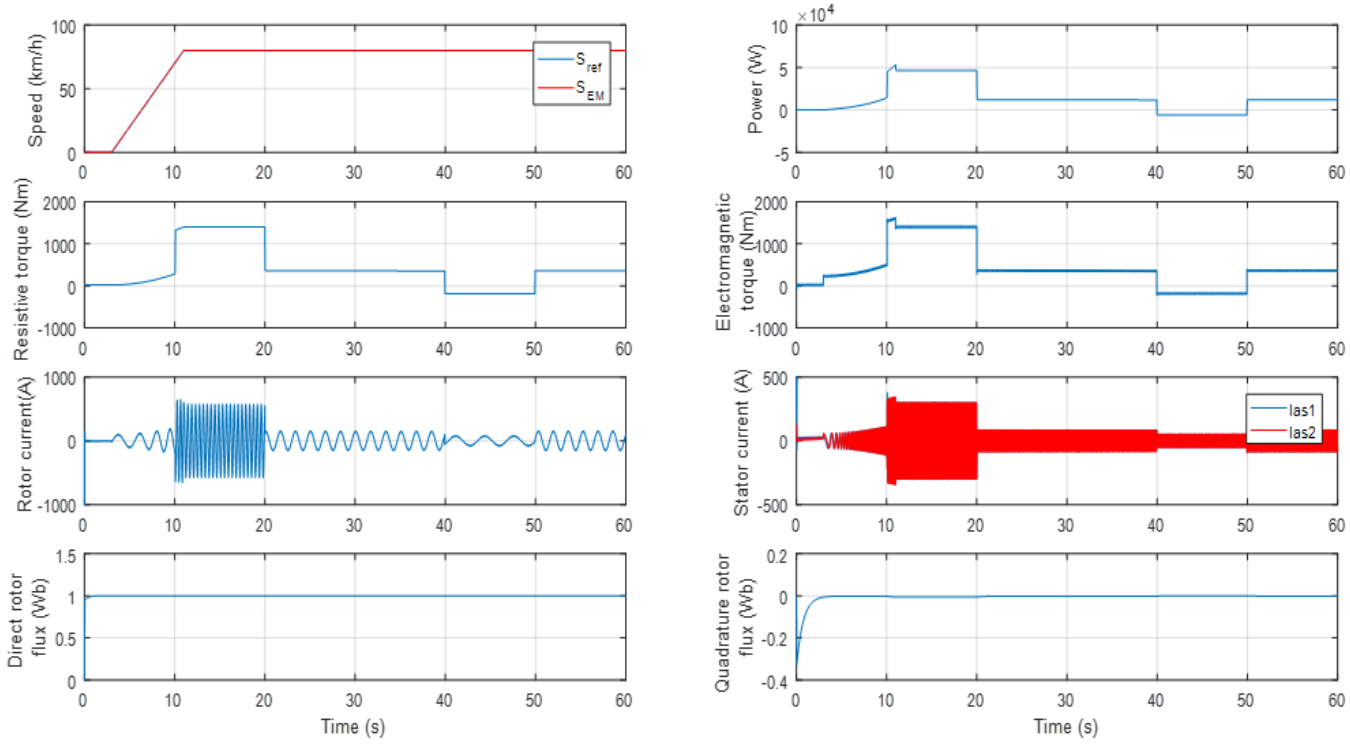

(**a**)

Figure 9. *Cont.*

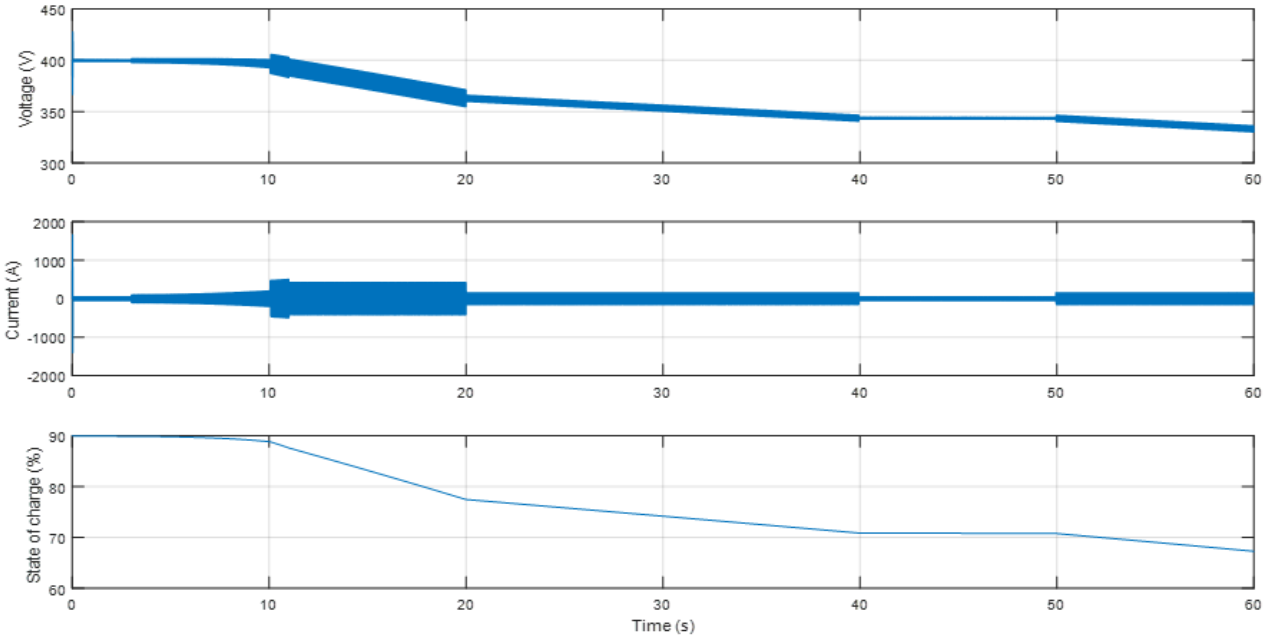

(**b**)

Figure 9. (**a**). Simulation results of test 4: Characteristic of the EV. (**b**). Simulation results of test 4: Characteristic of the battery.

The simulation results of this test show that overloading influences the electric vehicle driven by dual-star induction machine behavior on the two slopes of 30% and 15%, and this influence on the vehicle's traction can be seen in the increase in electromagnetic torque, which follows resistive torque directly after the vehicle's load is increased from 1300 kg to 2000 kg.

3.5. Simulation Results of Test 5: Speed Variation and Slope Variation

The aim of this test is to study the effectiveness of the robustness of the dual-star induction machine in the powertrain of an electric vehicle under sliding mode control in the various difficult conditions of speed and slope variation. To do this, we have provided a speed variation from 3 s to 52 with an ascending gradient of 30% from the second 10 s to the second 20 s, followed by a descending gradient of 15% and a speed variation from the second 40 s to the second 50 s.

The simulation results of this test under the Matlab Simulink environment are represented in Figure 10.

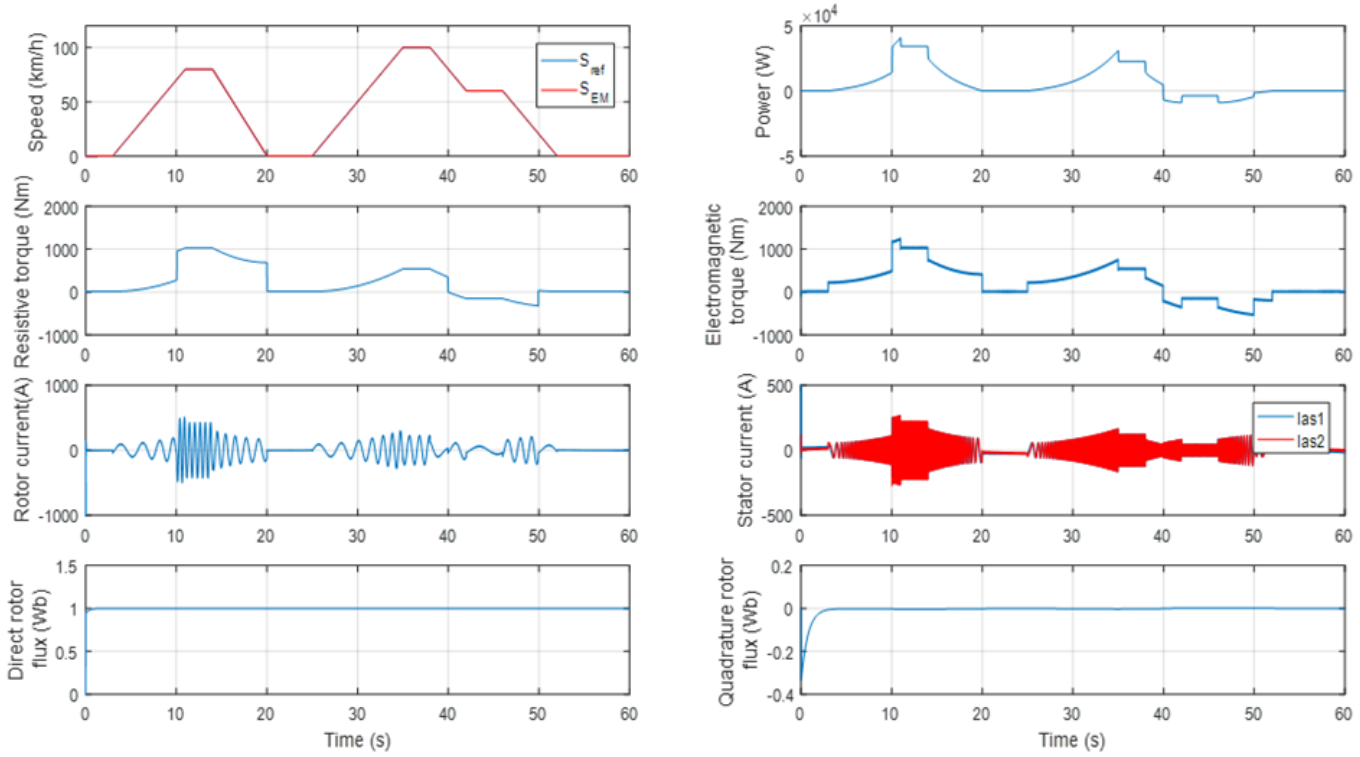

(**a**)

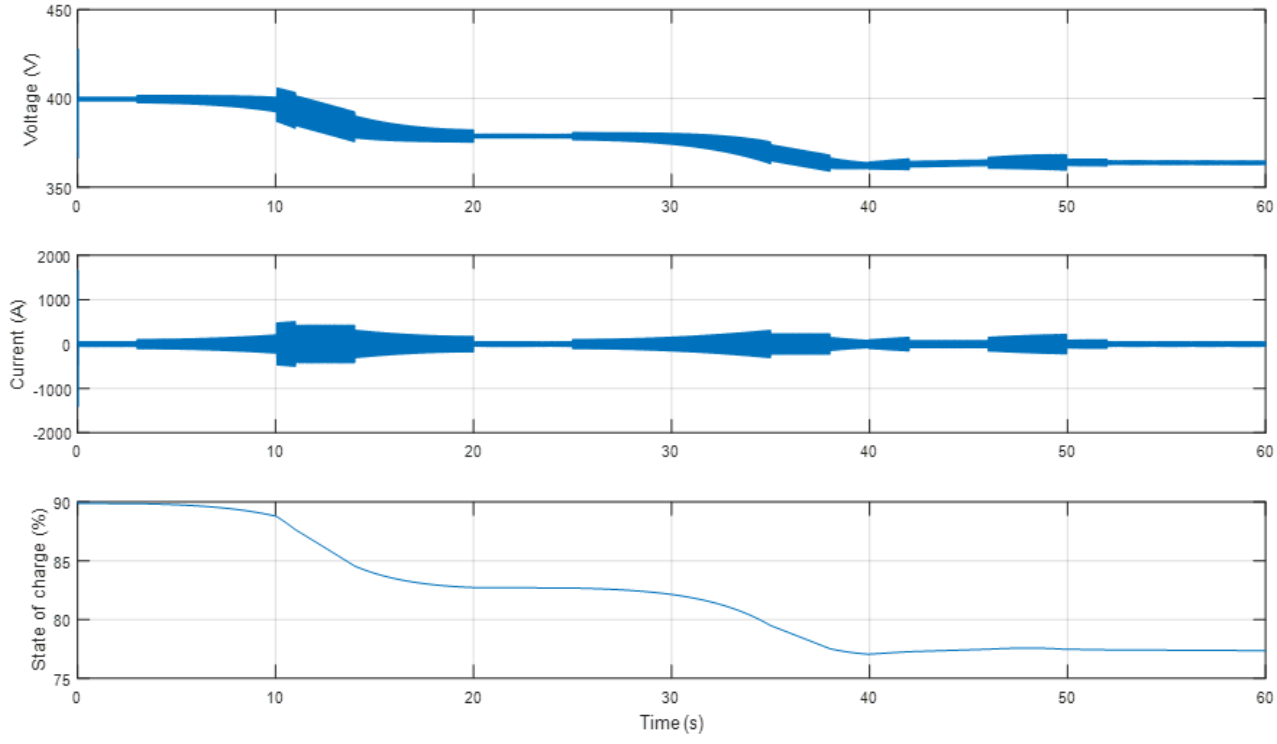

(**b**)

Figure 10. (**a**). Simulation results of test 5: Characteristic of the EV. (**b**). Simulation results of test 5: Characteristic of the battery.

The results of the simulation of the electric vehicle, confronted with variations in speed and gradient, highlight the major advantage of this type of powertrain: its ability to recover energy during braking phases or when driving downhill. This feature makes it a wise

choice, especially when driving in difficult conditions. Thanks to the use of a robust and efficient dual-star induction machine, the vehicle becomes capable of coping with adverse conditions such as steep inclines and wide fluctuations in speed. The strength of the drive machine thus plays a crucial role in ensuring the vehicle's reliability and performance in a variety of driving environments and situations.

3.6. Simulation Results of Test 6: Robustness Test

In this test, we demonstrate the robustness of the sliding mode control and the advantage of this control in electric vehicles. To do this, we applied a variation to the rotor resistance by decreasing it to 50 of its initial value from the second 10 and increasing it to 100 of its initial value from the second 30 with a variable speed and slope.

The simulation results of this test under the Matlab Simulink environment are represented in Figure 11.

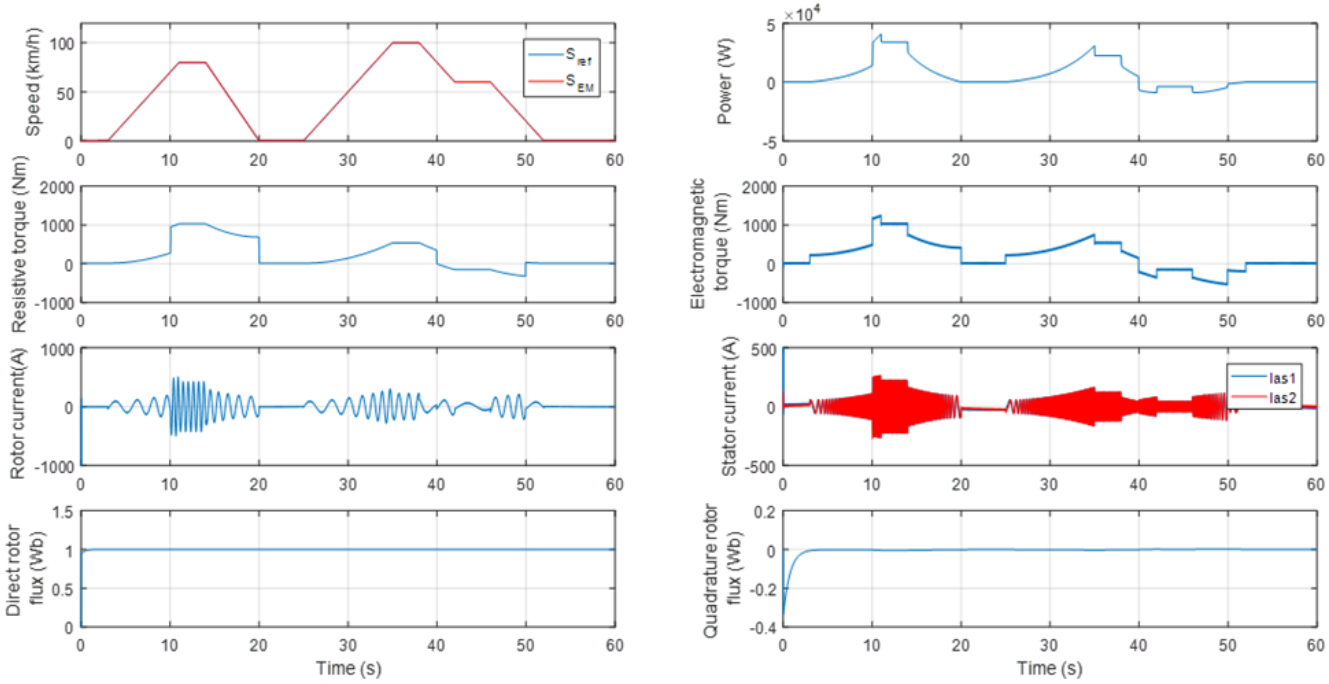

(**a**)

Figure 11. *Cont.*

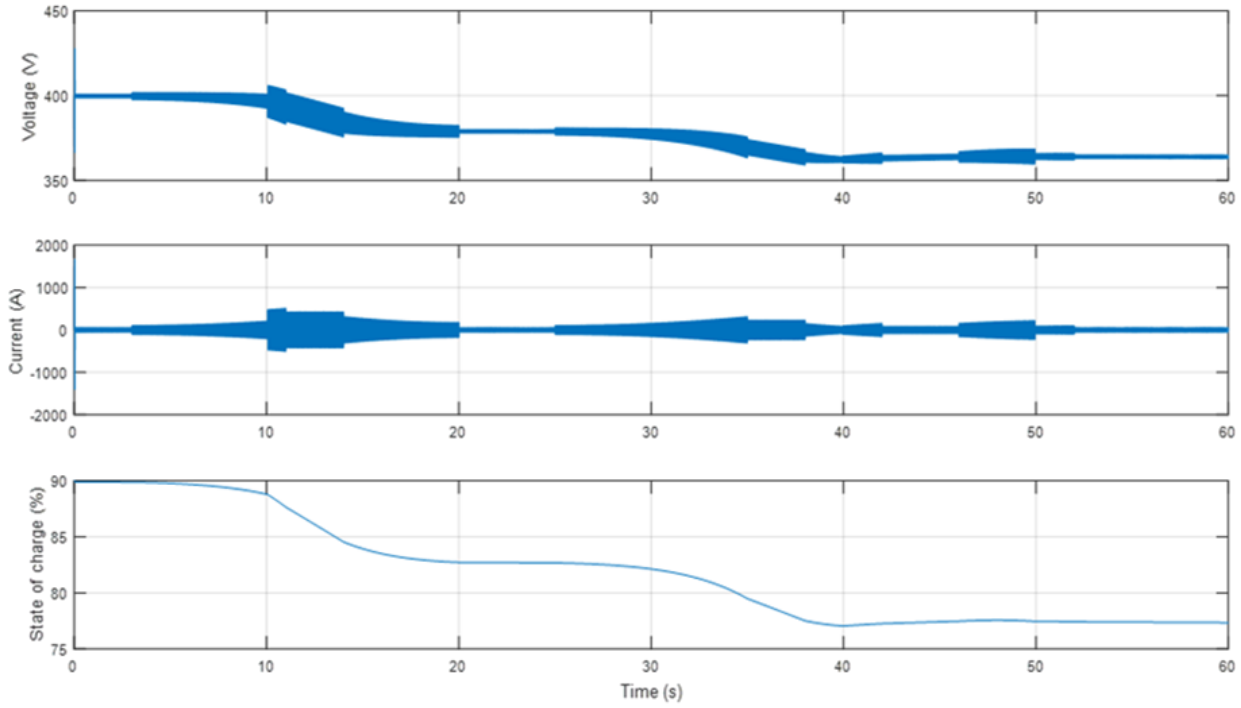

(**b**)

Figure 11. (**a**). Simulation results of test 6: Characteristic of the EV. (**b**). Simulation results of test 6: Characteristic of the battery.

The results of the simulated robustness test with the variation of the motor rotor resistance show the reliability and robustness of the sliding mode control used to drive the electric vehicle, bearing in mind the conditions under which the robustness tests were carried out. The mechanical load used is that of the vehicle with a variation in speed and gradient, with the two stars being identical.

Following this test, we carried out a performance study: dynamics, precision, and stability. We found that sliding-mode controllers are better than conventional controllers in every respect, apart from speed. They offer greater precision and stability and are less sensitive to external disturbances.

These results demonstrate the effectiveness and robustness of the sliding-mode control system for controlling and steering the electric vehicle's entire powertrain under different driver and road conditions.

4. Conclusions

The objective of this paper was to assess the efficiency of electric vehicle propulsion using a dual-star induction machine (DSIM). Our study aimed to comprehensively analyze the behavior and operation of this technology within the context of a four-quadrant vehicle, incorporating a lithium-ion battery as an energy source and three-level static converters. To achieve this, we implemented a control architecture based on a sliding mode control strategy, allowing us to effectively manage the vehicle's performance by adhering to a predefined driving cycle, thus ensuring optimal propulsion through the DSIM.

Simulations conducted in the Simulink/Matlab environment revealed that DSIMs are capable of delivering high torque from startup, which is crucial for the acceleration of electric vehicles. Furthermore, we observed that the reliability and durability of this technology could translate into a longer lifespan and reduced maintenance costs for electric vehicle owners, thereby contributing to the broader adoption of this technology.

It is important to highlight the richness and simplicity of sliding mode variable-structure control, which provides excellent dynamic responsiveness and a high capacity to precisely follow speed instructions. Additionally, this technology exhibits increased

resistance to disturbances caused by variations in external conditions, ensuring stable and reliable operation of the electric propulsion system in a variety of scenarios.

The use of DSIMs in the automotive industry, particularly in sports vehicles, represents a significant advancement in electric vehicle propulsion technology. DSIMs effectively meet all vehicle-specific performance objectives, such as efficiency, durability, and cost, thereby offering optimal performance and enhanced robustness, reinforcing their position as a preferred choice for the future of electric mobility.

This research proposal focuses on exploring innovative approaches in the development of electric vehicle propulsion systems. By adopting a practical and collaborative approach for our future research, the aim is to advance the technology of energy storage devices and new energy recovery technologies while integrating control systems leveraging artificial intelligence techniques. This approach could lead to the development of even more adaptive and efficient systems capable of dynamically adjusting to driving conditions and driver preferences, potentially positioning this proposal as a leading solution for the future of electric mobility. In this context, thorough experimental studies will be crucial in the future to verify the accuracy of these simulation models and evaluate the feasibility of integrating ESDs into real-world applications. This endeavor necessitates and requires close collaboration with the automotive industry to overcome the challenges associated with the production and commercialization of electric vehicles equipped with DSIMs.

Author Contributions: Conceptualization: B.B. and H.C.; methodology: B.B.; software: B.B., H.C. and Y.H.; validation B.B. and H.C.; formal analysis: B.B., D.C. and M.T.D.; investigation, B.B., M.A. and J.R.; resources, B.B., H.C., M.A. and J.R.; data curation: B.B. and H.C.; writing—original draft preparation: B.B., M.A. and J.R.; writing—review and editing: B.B., J.R. and M.A.; visualization: B.B., D.C. and M.T.D. supervision: H.C., J.R. and M.A. All authors have read and agreed to the published version of the manuscript.

Funding: This research received no external funding.

Data Availability Statement: The original contributions presented in the study are included in the article, further inquiries can be directed to the corresponding author/s.

Acknowledgments: J. Rodriguez acknowledges the support of ANID through projects FB0008, 1210208, and 1221293. The work of D. Chrenko has been supported by the EIPHI Graduate school (contract "ANR-17-EURE-0002") and by the Bourgogne-Franche-Comté Region.

Conflicts of Interest: The authors declare no conflicts of interest.

Abbreviations

EV	Electric vehicle
DSIM	Dual-star induction machine
p	Number of pole pairs
J	Total inertia of rotating parts
F	Network Frequency in 'Hz'
m	The total mass of the vehicle in 'kg'
g	The gravity in 'm/s^2'
β	The slope angle in 'rad/s'
α	The electrical angle in 'rad/s'
$pair$	The density of the air in 'kg/m^2'
$\boldsymbol{Af}$	The frontal area of the vehicle in 'm^2'
$\boldsymbol{r}$	Wheel radius 'm'
$\boldsymbol{Fres}$	The total resistive force in 'N'
$\boldsymbol{Tres}$	The resistant couple in 'Nm'
$\boldsymbol{Pev}$	The power of the electric vehicle in 'w'
$\boldsymbol{Vev}$	The speed of the vehicle in 'm/s^2'
$\boldsymbol{Vd, qs1}$	Voltages of star 1 in Park reference frame "d, q" in 'V'
$\boldsymbol{Vd, qs2}$	Voltages of star 2 in Park reference frame "d, q" in 'V'
$\boldsymbol{Vd, qr}$	Rotor voltages in Park reference frame "d, q " in 'V'

***id*, *qs*1**	Star 1 currents in the Park reference frame "d, q" in 'A'
***id*, *qs*2**	Star 2 currents in Park reference frame "d, q" in 'A'
id*, *qr	Rotor currents in Park reference frame "d, q" in 'A'
***φd*, *qs*1**	Flux of star 1 in Park reference frame "d, q" in 'wb'
***φd*, *qs*2**	Flux of star 2 in Park reference frame "d, q" in 'wb'
φd*, *qr	Rotor fluxes in the Park reference frame "d, q" in 'wb'
***Rs*1**	Stator resistances of the star 1 in 'Ω'
***Rs*2**	Stator resistances of the star 2 in 'Ω'
Rr	Rotor resistances in 'Ω'
Lm	Cyclic mutual inductance between star 1 and star 2 in 'H'
Lr	Rotor inductance in 'H'
LS	Stator inductance in 'H'
ia	Armature Current in 'A'
φf	Flux imposed by the excitation current in 'wb'
Cd	The aerodynamic drag coefficient
fro	The constant of the resistance force due to the displacement
G	Speed reducer
g	Sliding coefficient
K	Stator-rotor magnetic coupling coefficient
kpv*, *kiv	Proportional and integral gain of the speed controller.

References

1. Dalal, A.; Kumar, P. Design, Prototyping, and Testing of a Dual-Rotor Motor for Electric Vehicle Application. *IEEE Trans. Ind. Electron.* **2018**, *65*, 7185–7192. [CrossRef]
2. Sanguesa, J.A.; Torres-Sanz, V.; Garrido, P.; Martinez, F.J.; Marquez-Barja, J.M. A Review on Electric Vehicles: Technologies and Challenges. *Smart Cities* **2021**, *4*, 372–404. [CrossRef]
3. Yuvaraj, T.; Devabalaji, K.R.; Kumar, J.A.; Thanikanti, S.B.; Nwulu, N.I. A Comprehensive Review and Analysis of the Allocation of Electric Vehicle Charging Stations in Distribution Networks. *IEEE Access* **2024**, *12*, 5404–5461. [CrossRef]
4. Gao, W.; Peng, C.; Bao, W.; Wu, C. Communication energy optimization of electric vehicle platoon on curved road. *EURASIP J. Adv. Signal Process.* **2021**, *2021*, 105. [CrossRef]
5. Hussain, S.; Ahmed, M.A.; Kim, Y.-C. Efficient Power Management Algorithm Based on Fuzzy Logic Inference for Electric Vehicles Parking Lot. *IEEE Access* **2019**, *7*, 65467–65485. [CrossRef]
6. Fu, Z.; Zhu, L.; Tao, F.; Si, P.; Sun, L. Optimization based energy management strategy for fuel cell/battery/ultracapacitor hybrid vehicle considering fuel economy and fuel cell lifespan. *Int. J. Hydrogen Energy* **2020**, *45*, 8875–8886. [CrossRef]
7. Rimpas, D.; Kaminaris, S.D.; Aldarraji, I.; Piromalis, D.; Vokas, G.; Papageorgas, P.G.; Tsaramirsis, G. Energy management and storage systems on electric vehicles: A comprehensive review. *Mater. Today Proc.* **2022**, *61*, 813–819. [CrossRef]
8. Karmaker, A.K.; Hossain, M.A.; Pota, H.R.; Onen, A.; Jung, J. Energy Management System for Hybrid Renewable Energy-Based Electric Vehicle Charging Station. *IEEE Access* **2023**, *11*, 27793–27805. [CrossRef]
9. Vodovozov, V.; Raud, Z.; Petlenkov, E. Review on Braking Energy Management in Electric Vehicles. *Energies* **2021**, *14*, 4477. [CrossRef]
10. Huang, H.; Tu, Q.; Jiang, C.; Pan, M.; Zhu, C. An Electronic Line-Shafting Control Strategy Based on Sliding Mode Observer for Distributed Driving Electric Vehicles. *IEEE Access* **2021**, *9*, 38221–38235. [CrossRef]
11. Cao, W.; Bukhari, A.A.S.; Aarniovuori, L. Review of electrical motor drives for electric vehicle applications. *Mehran Univ. Res. J. Eng. Technol.* **2019**, *38*, 525–540. [CrossRef]
12. Cisse, K.M.; Hlioui, S.; Belhadi, M.; Rollet, G.M.; Gabsi, M.; Cheng, Y. Design optimization of multi-layer permanent magnet synchronous machines for electric vehicle applications. *Energies* **2021**, *14*, 7116. [CrossRef]
13. Hamitouche, K.; Chekkal, S.; Amimeur, H.; Aouzellag, D. A New Control Strategy of Dual Stator Induction Generator with Power Regulation. *J. Eur. Syst. Autom.* **2020**, *53*, 469–478. [CrossRef]
14. Lallouani, H.; Ssaad, B. Performances of type 2 fuzzy logic control based on direct torque control for double star induction machine. *Rev. Roum. Sci. Tech.-Ser. Electrotech. Energetique* **2020**, *65*, 103–108.
15. Liu, Y.; Liu, K.; Zhou, Y.; Chen, Y.; Wei, D.; Zhou, S.; Luan, H. Study on the Design and Speed Ratio Control Strategy of Continuously Variable Transmission for Electric Vehicle. *IEEE Access* **2023**, *11*, 107880–107891. [CrossRef]
16. Hassan, M.R.M.; Mossa, M.A.; Dousoky, G.M. Evaluation of Electric Dynamic Performance of an Electric Vehicle System Using Different Control Techniques. *Electronics* **2021**, *10*, 2586. [CrossRef]
17. Miao, Y.; Hynan, P.; von Jouanne, A.; Yokochi, A. Current Li-Ion Battery Technologies in Electric Vehicles and Opportunities for Advancements. *Energies* **2019**, *12*, 1074. [CrossRef]
18. Wang, Y.; Liu, C.; Pan, R.; Chen, Z. Modeling and state-of-charge prediction of lithium-ion battery and ultracapacitor hybrids with a co-estimator. *Energy* **2017**, *121*, 739–750. [CrossRef]

19. Timilsina, L.; Badr, P.R.; Hoang, P.H.; Ozkan, G.; Papari, B.; Edrington, C.S. Battery Degradation in Electric and Hybrid Electric Vehicles: A Survey Study. *IEEE Access* **2023**, *11*, 42431–42462. [CrossRef]
20. Schwenk, K.; Meisenbacher, S.; Briegel, B.; Harr, T.; Hagenmeyer, V.; Mikut, R. Integrating Battery Aging in the Optimization for Bidirectional Charging of Electric Vehicles. *IEEE Trans. Smart Grid* **2021**, *12*, 5135–5145. [CrossRef]
21. Sayed, K.; Almutairi, A.; Albagami, N.; Alrumayh, O.; Abo-Khalil, A.G.; Saleeb, H.A. Review of DC-AC Converters for Electric Vehicle Applications. *Energies* **2022**, *15*, 1241. [CrossRef]
22. Islam, R.; Rafin, S.H.; Mohammed, O.A. Comprehensive Review of Power Electronic Converters in Electric Vehicle Applications. *Forecasting* **2020**, *5*, 22–80. [CrossRef]
23. Jape, S.R.; Thosar, A. Comparison of electric motors for electric vehicle application. *Int. J. Res. Eng. Technol.* **2017**, *6*, 12–17. [CrossRef]
24. Azib, A.; Ziane, D.; Rekioua, T.; Tounzi, A. Robustness of the direct torque control of double star induction motor in fault condition. *Rom. J. Tech. Sci. Electr. Energy Eng. Ser.* **2016**, *61*, 147–152.
25. Tir, Z.; Soufi, Y.; Hashemnia, M.N.; Malik, O.P.; Marouani, K. Fuzzy logic field oriented control of double star induction motor drive. *Electr. Eng.* **2017**, *99*, 495–503. [CrossRef]
26. Chaabane, H.; Eddine, K.D.; Salim, C. Indirect self tuning adaptive control of double star induction machine by sliding mode. *Rev. Roum. Sci. Tech.-Ser. Electrotech. Energetique* **2019**, *64*, 409–415.
27. Ibrahim, N.; Abdelaziz, M.; Ghoneima, M.; Hammad, S. Implementation of vector control on electric vehicle traction system. *Bull. Natl. Res. Cent.* **2020**, *44*, 22. [CrossRef]
28. Xiu, C.; Wang, R. Sliding Mode Control Based on Dynamic Model for Transport Vehicle. *IEEE Access* **2018**, *6*, 33819–33825. [CrossRef]
29. Li, W.; Zhu, W.; Zhu, X.; Guo, J. Two-Time-Scale Braking Controller Design with Sliding Mode for Electric Vehicles over CAN. *IEEE Access* **2019**, *7*, 128086–128096. [CrossRef]
30. Layadi, N.; Djerioui, A.; Zeghlache, S.; Mekki, H.; Houari, A.; Gong, J.; Berrabah, F. Fault-tolerant control based on sliding mode controller for double-star induction machine. *Arab. J. Sci. Eng.* **2020**, *45*, 1615–1627. [CrossRef]